3D multiple attenuation and depth imaging of ocean bottom seismic data

Joachim Mispel, Børge Arntsen, Alexander Kritsky, Lasse Amundsen, Mark Thompson, Statoil, Ottar Sandvin and Leif Jahren, READ Well services*

SUMMARY

In 3D Ocean Bottom seismic surveys (3D-OBS) both pressure and vertical particle velocity is recorded. This presents the opportunity to decompose the recorded wavefields in up- and downgoing components and apply to 3D common receivers gathers a designature/demultiple algorithm to attenuate free surface multiples. This single processing step replaces several steps in conventional processing usually encompassing tau-p predictive deconvolution and Radon demultiple.
Using a 3D-OBS data set from the Gullfaks Sør field in the North Sea, the new 3D designature/demultiple approach, together with 3D common receiver depth migration, is shown to result in seismic images of better quality than by the traditional processing sequence.

INTRODUCTION

The major motivation in the early 1990's for going to the added effort and expense of placing the seismic sensing system on the ocean bottom was to record shear waves in addition to pressure waves to put petroleum seismologists in a better position to more reliably characterize the rock and its contained fluids than is possible from conventionally towed-streamer recordings (Berg et al., 1994a,b).

However, three-dimensional ocean bottom seismic (3D-OBS) surveys have other advantages and technical benefits compared to standard towed-streamer seismic surveys, which may be unsuitable for obtaining the very best reservoir images, especially in geologically complex areas. 3D-OBS - although more expensive - offers the distinct advantage of flexible acquisition geometries. Virtually any pattern of shots and receivers is possible with the aim of capturing the most revealing images. True 3D data acquisition is realized by using a stationary seabed sensing system combined with a survey vessel shooting over a predetermined grid on the sea surface. Every subsurface point on the target can thus be illuminated from all directions and a large number of angles during a 3D-OBS survey (Thompson et al., 2007).

To obtain accurate and detailed images, however, attenuation of multiple energy while preserving the character of primaries is required. By utilizing that the complete wavefield is recorded in the 3D-OBS experiment Amundsen et al. (2001) proposed an efficient deterministic designature/demultiple solution to the free-surface multiple problem that does not require any knowledge of the source signature nor the subsurface. The essence of the method is to design a demultiple operator from the inverse of the downgoing part of the acoustic wavefield (downgoing pressure or downgoing component of the particle velocity). In today's 3D-OBS surveys with dense source-side sampling but coarse cross-line receiver sampling the designature/demultiple method is run on 3D tau-p transformed common receiver gathers. The 3D tau-p transform is implemented as a discrete Radon transform that is rapidly computable and invertible by means of FFTs. Its basis is the concentric squares grid (Mersereau and Oppenheim, 1974) or the pseudo-polar grid (Averbuch et al., 2003) For most seismic applications, it is sufficient to transform data to a triangle subdomain of the concentric squares grid (Ikelle and Amundsen, 2005).

In the next two sections we review the basic theory of 3D designature/demultiple and 3D depth imaging of 3D-OBS data. Results of applying 3D designature/demultiple to 3D-OBS data from the Gullfaks Sør field in the North Sea is reviewed in the results section and shown to yield images of better quality than conventional multiple suppression techniques.

3D DEMULTIPLE/DESIGNATURE OF 3D-OBS DATA

Amundsen et al. (2001) derived an integral relationship between the recorded pressure and particle velocity data (p, v_m) in the *physical* ocean bottom seismic experiment, containing all free surface related multiples, and the desired designatured multicomponent data with those multiples absent, $(\tilde{p}, \tilde{v}_m)$. Here p is the pressure and v_m is the m'th component of the particle velocity. The desired data are those data that would be recorded in a *hypothetical* ocean bottom seismic experiment from a monopole or dipole point source with desired signature, $\tilde{a}$, in the case when the water layer extends upward to infinity. The geology below the water layer is the same in the physical and hypothetical ocean bottom seismic experiments.

Assume that the pressure field and the vertical component of the particle velocity (p, v_3) are acoustically decomposed into upgoing (u) and downgoing (d) waves so that the full fields always are the sum of their upgoing and downgoing components, according to

$$p = p^{(u)} + p^{(d)}; v_3 = v_3^{(u)} + v_3^{(d)}. \quad (1)$$

The following equation

$$\tilde{a} \cdot v_m(x_r, x_s) = -2i\omega\rho \int dx\, \tilde{v}_m(x_r, x) v_3^{(d)}(x, x_s) \quad (2)$$

then describes the integral relationship between the field $\tilde{v}_m$ in the *hypothetical* experiment, with point source of signature $\tilde{a}$ just above the sea floor and receivers at position x_r just below the sea floor, and the recorded *physical* field and computed downgoing component of the normal particle velocity just above the sea floor from a source located at center location x_s.

Pressure recordings are processed similarly. The integral relationship for the pressure fields in the physical and hypothetical experiments are

$$\tilde{a} \cdot p(x_r^-, x_s) = -2i\omega\rho \int dx\, \tilde{p}(x_r^-, x) v_3^{(d)}(x, x_s), \qquad (3)$$

where x_r^- denotes the hydrophone position just above the sea floor. Observe that $(-2i\omega\rho v_3^{(d)})^{-1}$ can be interpreted as a multidimensional operator that acts as (i) a deterministic designature operator, and (ii) a deterministic free-surface multiple attenuation operator. Since frequency domain multiplication by $-i\omega$ corresponds to temporal derivation, the operator is inversely proportional to the time derivative of $v_3^{(d)}$.

Note that no information, except location, about the physical source array and its wavelet, and no information of the properties of the water layer above the recording plane has been used to derive the integral equations for $\tilde{v}_m$ and $\tilde{p}^{(u)}$. Hence, the method is independent of volume and geometry of the marine source array and independent of any vertical variations in water layer properties and the state of the sea surface. This property potentially can make the method attractive for processing time-lapse ocean bottom seismic data. The integral equations are Fredholm integral equations of the first kind for the desired designatured/demultipled fields, leading to a system of equations that can be solved for $\tilde{v}_m$ and $\tilde{p}^{(u)}$ by keeping the receiver coordinate fixed while varying the source coordinate.

Designature/Demultiple Method for Layered Earth

In a horizontally layered medium the seismic response is laterally shift invariant with respect to source location. It then follows that any component of the designatured/demultipled field is obtained by spectral deconvolution between the field itself and the downgoing part of the pressure. In the frequency-wavenumber domain the designature/demultiple of the *m*th component of the particle velocity reads (Amundsen et al., 2004)

$$\tilde{V}_m = \frac{V_m}{P^{(D)}} \tilde{P}^{(dir)}, \qquad (4)$$

while the designature/demultiple of the upgoing pressure recording becomes

$$\tilde{P}^{(U)} = \frac{P^{(U)}}{P^{(D)}} \tilde{P}^{(dir)} \qquad (5)$$

where, for a monopole point source,

$$\tilde{P}^{(dir)} = -\frac{\tilde{a}}{2ik_z} \exp[ik_z(z_r - z_s)] \qquad (6)$$

or, for a dipole point source,

$$\tilde{P}^{(dir)} = -\frac{\tilde{a}}{2} \exp[ik_z(z_r - z_s)] \qquad (7)$$

is the direct wavefield from the desired source. The phase shift corrects for difference in source and receiver depth levels, and k_z is the vertical wavenumber. Observe that$(P^{(D)})^{-1}$ is the multidimensional spiking deconvolution operator. This designature/demultiple scheme may be implemented as frequency-wavenumber domain or tau-p domain algorithms. In the frequency-wavenumber domain, a joint designature and multiple attenuation process is performed for each combination of frequency and wavenumber. In the tau-p domain, the process is performed for each p-trace. White noise can be added to stabilize the deconvolution. The amount of added white noise can vary as function of slowness. In today's 3D4C-OBS surveys with dense source-side sampling but coarse cross-line receiver sampling the designature/demultiple method is run on tau-p transformed common receiver gathers. Compared to published techniques for 3D free-surface demultiple for streamer data, this designature/demultiple method is very fast. To our knowledge, this is the only deterministic free-surface demultiple method that directly can be applied to 3D4C-OBS surveys with today's geometries.

3D COMMON RECEIVER DEPTH MIGRATION

Most prestack depth migration algorithms can be expressed as a wave field extrapolation step followed by an imaging condition. In our case, the primary reflection data p is approximated with the demultipled upgoing pressure $p \approx \tilde{p}^{(u)}$. Using the frequency-wavenumber formulation given in the preceding section, the demultipled upgoing pressure can be computed independently for each common receiver gather. By using reciprocity we can replace the common receiver gather with a common source gather, where the 3D-OBS receiver becomes the source, and the sources becomes new receivers. In this way we can use Claerbouts shot-profile approach for imaging 3D-OBS compressional waves.

The wave field extrapolation step can be derived from the Kirchhoff integral

$$p(x, \omega) = \int_S d\mathbf{S} \cdot \nabla g^*(x, x_r, \omega)\; p(x_r, \omega), \qquad (8)$$

where x denotes position $x = (x_1, x_2, x_3)$ and ω the angular frequency, while $p(x, \omega)$ is the extrapolated wave field at depth. The integral extends over the receiver surface S and $p(x_r, \omega)$ is data recorded at the receiver position x_r, while $g(x, x_r, \omega)$ is the Greens function.

The source wavefield s is also given by the Kirchhoff integral as

$$s(x, \omega) = \int_{S'} d\mathbf{S}' \cdot \nabla g(x, x_s, \omega)\; s(x_s, \omega), \qquad (9)$$

where S' is a surface where the initial source wavefield is specified. In our case this is a horizontal surface at the depth of the source.

The approximation for the Greens function used in wave equation finite-difference prestack depth migration is

$$g(x, x_r, \omega) = \exp[-ikr(x, x_r)]/r(x, x_r), \qquad (10)$$

where $r(x, x_s)$ is the distance from point x to point x_s, $k = \omega/c(x)$ is the wavenumber, and $c(x)$ is the velocity (Hale, D., 1991; Sollid and Arntsen, 1994). The Greens function in (10) is strictly speaking only valid for constant velocity, but by implementing the Kirchhoff integral in (8) recursively in depth and assuming that the velocity model is locally smooth, laterally inhomogeneous velocity fields can be handled. Our implementation uses a numerically optimized technique for the wave equation finite-difference extrapolation operators as suggested by Mittet, R. (2001)

$$p(x_1,x_2,x_3+\Delta x_3,\omega) = \sum_{i,j=-l_x,l_y}^{lx,ly} w(x_1-i\Delta x_1,x_2-j\Delta x_2,\omega/c(x)) \times p(i\Delta x_1, j\Delta x_2,x_3,\omega). \quad (11)$$

Here Δx_1 and Δx_2 are the sampling intervals in the two horizontal directions, while Δx_3 is the depth sampling interval and lx, ly are the half-length of the migration operator. w is a band-limited approximation to the the gradient of the green's function in (10) with a Fourier-transform given by

$$W(k_z,\omega) = exp(ik_z\Delta x_3)F(kz), \quad (12)$$

where F is a smooth windowing function ensuring that the magnitude of W is equal to unity for real vertical wavenumber k_z and approaches zero when k_z becomes imaginary.

Wave field extrapolation is done separately for the data and the source wave field and an image $r(x)$ is obtained by cross correlation of the two extrapolated wave fields

$$r(x) = \int d\omega p(x,\omega)s^*(x,\omega). \quad (13)$$

DEMULTIPLE AND IMAGING OF THE GULLFAKS SØR 3D-OBS DATA

The Gullfaks Sør field is located in the Norwegian sector of the North Sea and was discovered in 1978. A 3D-OBS survey was acquired in 2002, with a layout consisting of 16 cables separated by 400 meters. Each cable contained receivers with a group distance of 25 meters. The shot area is effectively a 50 by 50 meter grid covering the same area as the cable layout with 6 kilometers additional coverage in the inline direction and 2 kilometer extra coverage in the cross-line direction.

The main steps of the initial pre-processing of the data consisted of PZ-summation, deconvolution and noise-removal in the tau-p domain and an extra pass of Radon demultiple to remove remaining multiples. 3D common receiver depth migration using the approach described in the previous section was then applied with an already existing velocity model and a maximum frequency of 28 Hz. Post-processing included only amplitude scaling with time, trace-balancing, and stretching of the depth-axis back to time. Figures 1(a) and 2(a) show two inlines from the final stack.

The raw data were then reprocessed using the designature / demultiple approach described in the first section, implemented assuming a layered earth model in the tau-p domain. The multidimensional spiking deconvolution operator was computed from amplitude-frequency and phase-frequency matched pressure and vertical component of particle velocity. The desired source signature chosen was a zero-phase wavelet. The same 3D common receiver depth imaging algorithm as described above with identical velocity model was also applied.

Figures 1 and 2 show a comparison between the two inlines processed with conventional demultiple techniques described above and the same two inlines processed using designature / demultiple. The change in quality is noticeable; in particular is the Base Cretaceous unconformity between 2.6 and 2.7 seconds of two-way time much better defined on the lines processed with the designature/demultiple technique. Also strong multiples in the overburden and below 3.0 seconds are apparently removed. In general, the inlines processed using the designature/deconvolution approach are less noisy and contain reflectors with better continuity in the target area.

CONCLUSIONS

A new and simpler processing sequence for 3D-OBS data has been presented. The sequence fundamentally contains only two major steps: Preprocessing using 3D designature / demultiple followed by 3D common receiver depth imaging. The 3D designature/demultiple stage does not need any information about the source array (except location), about the sea floor parameters and the subsurface below the sea floor, about any variations in the water layer from the local density and acoustic velocity, or about the state of the sea surface. Implicitly in the demultiple process is a designature process that removes the source array effects from the recorded data. Also using the layered earth assumption, the demultiple/designature can be applied very efficiently to each separate common receiver gather individually. There is no need for expensive data-reordering and combination steps.

The imaging step of the processing sequence consists of 3D depth migration and is applied directly to each individual common receiver gather. An explicit finite-difference migration algorithm is used, which is cost-effective due to the large number of traces in each gather.

Because the overburden down to the Base Cretaceous level does not show significant lateral variation we find that the layered model designature/demultiple scheme works satisfactorily on 3D-OBS seismic data. The P-wave depth sections from the Gullfaks Sør seismic survey show that the designature / demultiple algorithm provides images with less multiples and better continuity of target reflectors than the conventional multiple attenuation approach.

ACKNOWLEDGMENTS

We thank Statoil ASA for allowing us to publish this result.

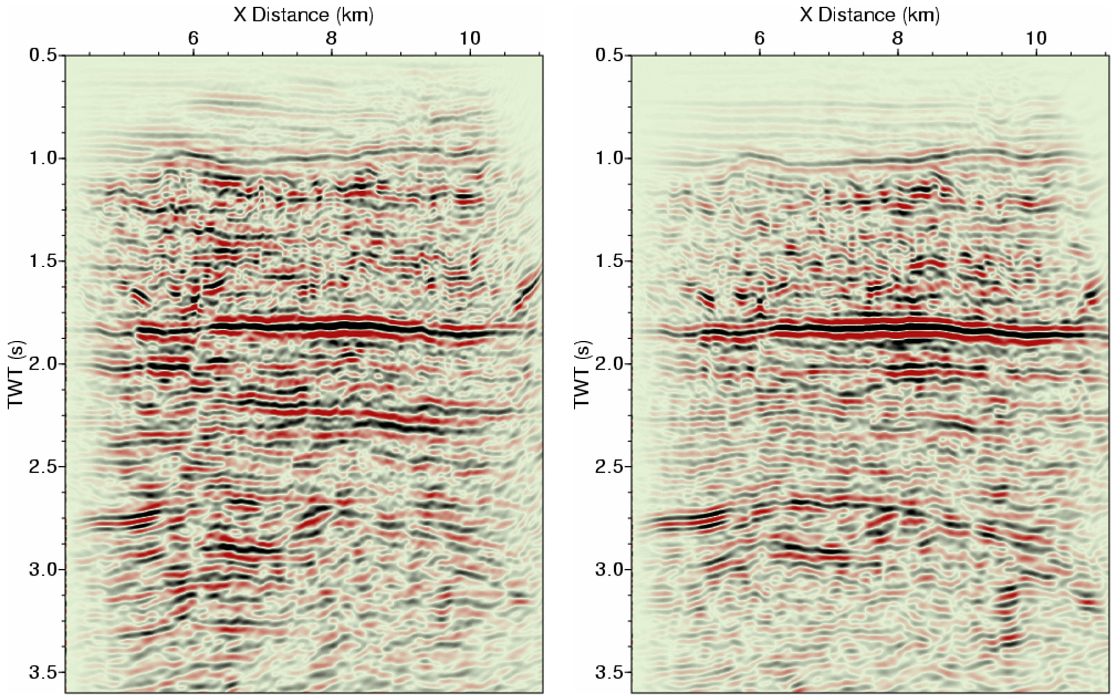

(a) (b)

Figure 1: (a) A 3D-OBS inline with conventional demultiple techniques and (b) the same inline with designature/demultiple applied.

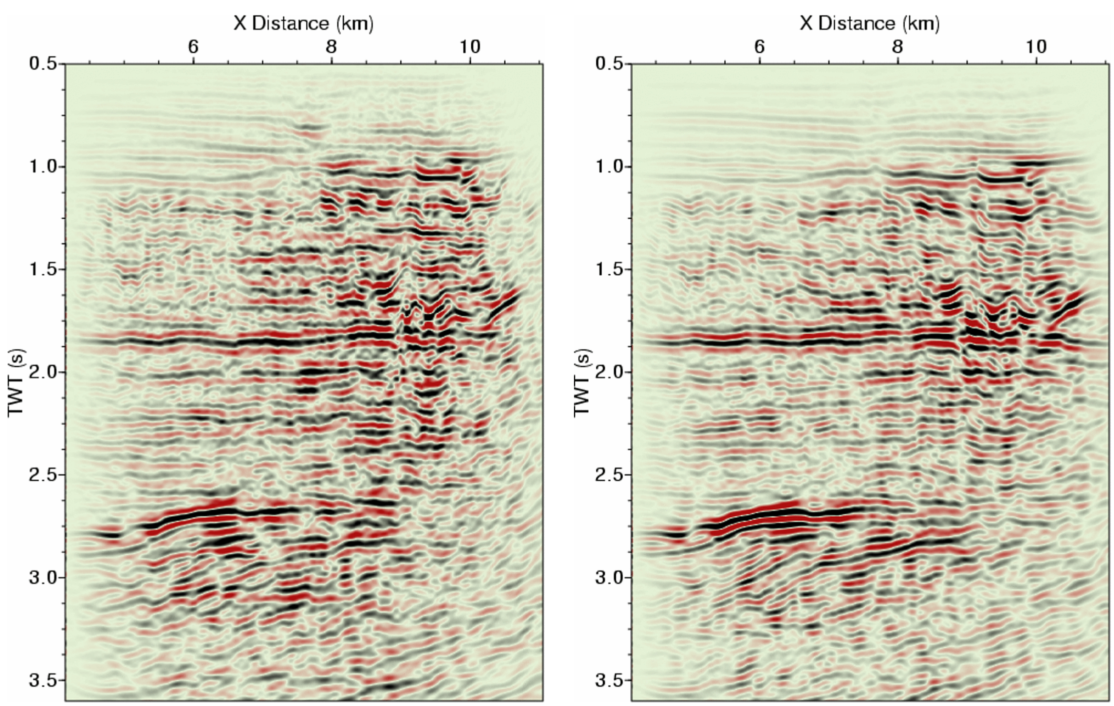

(a) (b)

Figure 2: (a) A second line from the same 3D-OBS dataset with conventional demultiple processing. (b) The same inline as in (a) but using designature/demultiple processing

EDITED REFERENCES

Note: This reference list is a copy-edited version of the reference list submitted by the author. Reference lists for the 2007 SEG Technical Program Expanded Abstracts have been copy edited so that references provided with the online metadata for each paper will achieve a high degree of linking to cited sources that appear on the Web.

REFERENCES

Amundsen, L., B. Arntsen, H. Aronsen, A. Osen, G. Richardsen, and M. Thompson, 2004, Fast deterministic designature/demultiple of 2D and 3D 4C-OBS data: Offshore Technology Conference, Expanded Abstracts.

Amundsen, L., L. Ikelle, and L. Berg, 2001, Multidimensional signature deconvolution and free-surface multiple elimination of marine multicomponent ocean-bottom seismic data: Geophysics, 66, 1594–1604.

Averbuch, A., R. Coifman, D. L. Donoho, and M. Israeli, 2003, Fast slant stack: A notion of radon transform for data in a cartesian grid which is rapidly computible, algebraic exact, geometrically faithful and inverible, http://students.som.yale.edu/phd/jpw29/fastradon042001.pdf.

Berg, E., B. Svenning, and J. Martin, 1994a, SUMIC — A new strategic tool for exploration and reservoir mapping: 56th Annual International Meeting, EAGE, Expanded Abstracts.

———, 1994b, SUMIC — Multicomponent sea-bottom seismic surveying in the North Sea — Data interpretation and applications: 54th Annual International Meeting, SEG, Expanded Abstracts, 1109–1116.

Hale, D., 1991, 3-D depth migration via McClellan transformations: Geophysics, 56, 1778–1785.

Ikelle, L., and L. Amundsen, 2005, Introduction to petroleum seismology: SEG.

Mersereau, R. M., and A. V. Oppenheim, 1974, Digital reconstruction of multidimensional signals from their projections: IEEE, 62, 1319–1338.

Mittet, R., 2002, Explicit 3D depth migration with a constrained operator: 72nd Annual International Meeting, SEG, Expanded Abstracts, 1148–1151.

Sollid, A., and B. Arntsen, 1994, Cost-effective 3D one-pass depth migration: Geophysical Prospecting, 42, 755–776.

Thompson, M., B. Arntsen, and L. Amundsen, 2007, Experiences with full azimuth acquisition in ocean bottom seismic: First Break, 25, 77–84.